Quantum correlations and entanglement in a model comprised of a short chain of nonlinear oscillators

J. K. Kalaga,[1] A. Kowalewska-Kudłaszyk,[2] W. Leoński,[1] and A. Barasiński[1]

[1]*Quantum Optics and Engineering Division, Faculty of Physics and Astronomy, University of Zielona Góra, Prof. Z. Szafrana 4a, 65-516 Zielona Góra, Poland*

[2]*Nonlinear Optics Division, Faculty of Physics, Adam Mickiewicz University, Umultowska 85, 61-614 Poznań, Poland*

(Received 4 December 2015; published 2 September 2016)

We discuss a model comprised of a chain of three Kerr-like nonlinear oscillators pumped by two modes of external coherent field. We show that the system can be treated as nonlinear quantum scissors and behave as a three-qubit model. For such situation, different types of tripartite entangled states can be generated, even when damping effects are present in the system. Some amount of such entanglement can survive even in a long-time limit. The flow of bipartite entanglement between subsystems of the model and relations among first-order correlations, second-order correlations, and the entanglement are discussed.

DOI: 10.1103/PhysRevA.94.032304

I. INTRODUCTION

Quantum correlations, including quantum entanglement, seems to be one of the most intriguing problems of contemporary physics. Such correlations play a crucial role not only in searching for the answers to the most fundamental questions concerning laws ruling quantum reality, but also in more practical applications such as those related to quantum information theory. As the bipartite entanglement and other forms of quantum correlations seem to be well understood, such correlations in systems containing three and more subsystems still need thorough investigation. Therefore, finding physical models that are helpful in the research in this field and, on the other side, that are general enough to be applied in various physical realizations is a very important problem.

Good candidates for such models are those involving quantum Kerr-like nonlinear oscillators. The effective Hamiltonians describing such systems involve terms with third-order susceptibilities (Kerr-like nonlinearities). Quantum Kerr-like models are widely discussed in numerous applications. For instance, they were considered as a source of non-Gaussian motional states of trapped ions [1] and of the superposition of coherent states [2,3], and were discussed in the context of Bell's inequality violations [4]. Moreover, Kerr-like oscillatory models were the subject of numerous papers related to quantum chaos problems (for instance, see [5]).

Importantly, models described by the Hamiltonians involving Kerr-type nonlinearities can be found in various, not necessarily optical, physical systems. Such nonlinearities are applied in the description of nanomechanical resonators and various optomechanical systems [6–11], boson trapped lattices [12–14], Bose-Einstein condensates [15], Bose-Hubbard chains [14,16], and in circuit QED models [17,18] (also involving superconducting systems [19]).

One of the key problems related to quantum information theory is quantum state engineering allowing for the finite-dimensional states' generation. Such states can also exhibit such interesting properties as the ability to produce various kinds of quantum correlations, including quantum entanglement. Physical systems involving at least two separate components characterized by the third-order susceptibilities (Kerr-like nonlinearities) are those which allow for the creation of such quantum states. Although such multimode systems can be found in various physical situations, they are referred to as Kerr-like couplers—their evolution is governed by the same effective Hamiltonians as the usual optical Kerr couplers (a discussion of such optical systems can be found, for instance, in [20], including review paper [21]).

As it was shown in [22], Kerr-like couplers can be treated as *nonlinear quantum scissors* (NQS) [23]. NQS systems exhibit such evolution for which only some limited number of n-photon states is involved. After such truncation of the wave function, a coupler playing the NQS role can be treated as a two-qubit [22], two-qutrit [22], or qutrit-qubit [22] model. It was also shown there that various maximally entangled states can be generated by such systems, including not only the usual Bell states but also generalized ones [24].

In fact, in NQS models, we observe so-called photon (phonon) blockade effects. At this point, one should mention that such effects have also been widely discussed. For instance, they have been observed in systems involving an optical cavity with a trapped atom (Caltech experiment [25]), a quantum dot coupled to a photonic crystal resonator (Stanford experiment [26]), a superconducting qubit coupled to a transmission-line resonator (ETH-Zurich experiment [27]), and in a superconducting circuit (Princeton-NIST experiment [19]). Moreover, quite recently, an experiment with a microwave cavity coupled to the superconducting qubit was performed [28].

Kerr-like oscillators were also discussed in the context of various special quantum states appearing in the tripartite systems. For instance, three nonlinear oscillators mutually coupled to each other were used as a source of entangled W states [29]. It is particularly important because recently tripartite and multipartite entanglement have become one of the most intriguing features discussed in the literature (for instance, see [15,30]).

The main aim of the present paper is to show how various types of quantum correlations can appear during the evolution of a chain of Kerr-like oscillators externally pumped by coherent fields. In particular, we are interested in the generation of tripartite entangled states belonging to various classes. It appears that for such system, during its evolution, depending

 ©2016 American Physical Society

on the strengths of the internal and external coupling strengths, Greenberger-Horne-Zeilinger (GHZ), W, and other types of entangled tripartite states can be generated. Moreover, we show that bipartite entangled states are generated not only for the subsystem involving two directly interacting oscillators, but also for oscillators interacting only via the third one. The degree of this entanglement is not fragile to the internal interactions strength. To check how the quantum correlations discussed are fragile for dissipation effects, the dynamics of a Kerr-type chain is also studied for the two models of external reservoirs: amplitude- and phase-damping ones. It appears that in the amplitude-damping reservoir in the steady-state limit, even for relatively large damping constants, some amount of tripartite entanglement can be left in the system.

In the literature, we can find discussion concerning problems of relations among the correlation functions (of the first and second order) and entanglement obtained in various quantum systems, such as atomic ensembles in high-Q cavities [31] or some optomechanical systems [32]. It was shown there that the entanglement is sensitive to the first-order coherence between the studied modes and that they are not simultaneously present in the system. The problem of such relation for the tripartite system will also be discussed in the present paper. We shall also focus on the second-order correlation function with reference to both two- and tripartite entanglement.

II. THE MODEL AND SOLUTIONS

We discuss a model of three identical nonlinear Kerr-like quantum oscillators. They are coupled to each other by linear interaction and form a chain of oscillators (see Fig. 1)—one central oscillator and two boundary ones. Moreover, two of them (boundary oscillators) are excited by an external coherent field. The system is governed by the following effective Hamiltonian:

$$\hat{H} = \hat{H}_{\rm nl} + \hat{H}_i + \hat{H}_e, \tag{1}$$

where

$$\hat{H}_{\rm nl} = \frac{\chi}{2}(\hat{a}_1^\dagger)^2\hat{a}_1^2 + \frac{\chi}{2}(\hat{a}_2^\dagger)^2\hat{a}_2^2 + \frac{\chi}{2}(\hat{a}_3^\dagger)^2\hat{a}_3^2 \tag{2}$$

describes the free evolution of the oscillators, and

$$\hat{H}_i = (\varepsilon\hat{a}_1^\dagger\hat{a}_2 + \varepsilon^*\hat{a}_2^\dagger\hat{a}_1) + (\varepsilon\hat{a}_2^\dagger\hat{a}_3 + \varepsilon^*\hat{a}_3^\dagger\hat{a}_2) \tag{3}$$

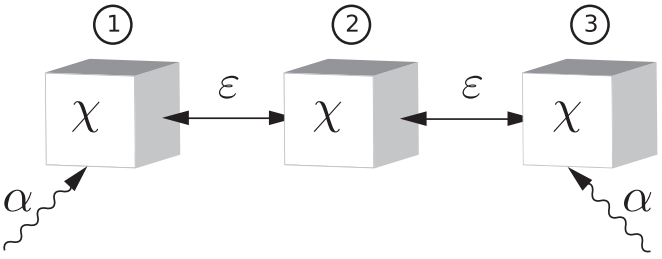

FIG. 1. Scheme of the model. A chain of nonlinear oscillators which are coupled mutually by linear interaction of the strength ε. Two (boundary) oscillators are excited by an external coherent field (the coupling strength is labeled α).

represents the internal interaction within pairs of two subsequent oscillators ($1-2$ and $2-3$), whereas

$$\hat{H}_e = \alpha\hat{a}_1^\dagger + \alpha^*\hat{a}_1 + \alpha\hat{a}_3^\dagger + \alpha^*\hat{a}_3 \tag{4}$$

describes the interaction with the external field. The operators $\hat{a}_j^\dagger$ and $\hat{a}_j$ ($j = 1,2,3$) are bosonic creation and annihilation operators corresponding to the three modes 1, 2, and 3, respectively. The parameter ε describes the strengths of linear couplings between modes $1-2$ and $2-3$, where we assume that both couplings ($1-2$ and $2-3$) are equal to each other, and the parameter ε is assumed to be real, i.e., ($\varepsilon = \varepsilon^*$). The strengths of the excitations of oscillators 1 and 2 by an external field are identical and are described by α, where $\alpha = \alpha^*$. We deal here with bosonic systems commonly applied in quantum optics. Nevertheless, it is worth noting that nontrivial coupling between the boson's degree of freedom can also be important in condensed-matter physics, where the superconducting state is often observed (for instance, see [33]).

To describe the system's evolution for the case when damping effects are neglected, we shall apply the standard Schrödinger-equation solution method. Therefore, we define the following three-mode wave function defined in an n-photon Fock states basis:

$$\begin{aligned}|\psi(t)\rangle &= \sum_{i,j,k=0}^{\infty} C_{ijk}(t)|i\rangle_1 \otimes |j\rangle_2 \otimes |k\rangle_3 \\ &\equiv \sum_{i,j,k=0}^{\infty} C_{ijk}(t)|ijk\rangle,\end{aligned} \tag{5}$$

where C_{ijk} are complex probability amplitudes corresponding to the states $|ijk\rangle$.

If we assume that external excitation and coupling between oscillators are weak if compared to the nonlinearity parameters ($\alpha,\varepsilon \ll \chi$), then the system's evolution remains closed within a finite set of n-photon states. For such situation, the system behaves as *nonlinear quantum scissors* (NQS) (for instance, see [34] and review paper [23]) and its wave function is defined in finite-dimensional Hilbert space [35]. What is interesting is that the NQS effect is, in fact, equivalent to the *photon (phonon) blockade* [9,19,25,36]. For the situation discussed here, we also assume that the system's evolution starts from the vacuum state $|000\rangle$ and hence it is limited to only eight states $|ijk\rangle$, $i,j,k \in \{0,1\}$. Consequently, the truncated wave function can be expressed in the following form:

$$\begin{aligned}|\psi(t)\rangle_{\rm cut} = {} & C_{000}(t)|000\rangle + C_{001}(t)|001\rangle + C_{010}(t)|010\rangle \\ & + C_{011}(t)|011\rangle + C_{100}(t)|100\rangle + C_{101}(t)|101\rangle \\ & + C_{110}(t)|110\rangle + C_{111}(t)|111\rangle.\end{aligned} \tag{6}$$

Such cutting of Hilbert space, and hence the wave function, is related to the fact that the Hamiltonian (2) generates unevenly spaced energy levels, where the vacuum and one-photon states are degenerate, with their energies equal to zero. For the situation considered here, those states are resonantly coupled to each other by weak, zero-frequency couplings, and are dominant in the system's evolution. To describe the contribution of two- (and more) photon states, we need higher-order perturbative solutions (see [37]). Then, applying the standard procedure, we find equations of motion for our

system's dynamics. As $|\psi(t=0)\rangle = |000\rangle$, these equations lead to the following formulas determining the time evolution of the probability amplitudes:

$$
\begin{aligned}
C_{000}(t) &= \frac{1}{8\alpha^4+2\varepsilon^4}\{4\alpha^4 - 2\alpha^2\varepsilon^2 + 2\varepsilon^4 \\
&\quad + \alpha^2[A_1\cos(\omega_1 t) + A_2\cos(\omega_2 t)]\}, \\
C_{001}(t) &= C_{100}(t) = \frac{-i\alpha}{2}\left[\frac{\sin(\omega_1 t)}{\omega_1} + \frac{\sin(\omega_2 t)}{\omega_2}\right], \\
C_{010}(t) &= \frac{\alpha}{8\alpha^4+2\varepsilon^4}[-2\varepsilon^3 + A_3\cos(\omega_1 t) + A_4\cos(\omega_2 t)], \\
C_{011}(t) &= C_{110}(t) = \frac{-i\alpha}{2}\left[\frac{\sin(\omega_1 t)}{\omega_1} - \frac{\sin(\omega_2 t)}{\omega_2}\right], \\
C_{101}(t) &= \frac{\alpha}{8\alpha^4+2\varepsilon^4}[-4\alpha^3 + 2\alpha\varepsilon^2 + A_3\cos(\omega_1 t) \\
&\quad + A_5\cos(\omega_2 t)], \\
C_{111}(t) &= \frac{\alpha^2}{8\alpha^4+2\varepsilon^4}[4\alpha\varepsilon + A_1\cos(\omega_1 t) - A_2\cos(\omega_2 t)],
\end{aligned}
\tag{7}
$$

where two frequencies ω_1 and ω_2 are defined as

$$
\begin{aligned}
\omega_1 &= \sqrt{4\alpha^2 + 4\alpha\varepsilon + 2\varepsilon^2}, \\
\omega_2 &= \sqrt{4\alpha^2 - 4\alpha\varepsilon + 2\varepsilon^2},
\end{aligned}
\tag{8}
$$

and we have defined the following parameters:

$$
\begin{aligned}
A_1 &= 2\alpha^2 - 2\alpha\varepsilon + \varepsilon^2, \quad A_2 = 2\alpha^2 + 2\alpha\varepsilon + \varepsilon^2, \\
A_3 &= 2\alpha^3 - \alpha\varepsilon^2 + \varepsilon^3, \quad A_4 = -2\alpha^3 + \alpha\varepsilon^2 + \varepsilon^3, \\
A_5 &= 2\alpha^3 - \alpha\varepsilon^2 - \varepsilon^3.
\end{aligned}
\tag{9}
$$

What should be emphasized is that although the nonlinearity constant χ does not appear here as a result of the fact that eigenenergies corresponding to the vacuum and one-photon states are equal to zero, the process of cutting of the wave function requires the presence of the nonlinearity.

We see that two frequencies ω_1 and ω_2 appear in our solution. To get regular and periodic solutions, we have to choose the values of these frequencies carefully and concentrate on the cases for which the ratio between them fulfills some special conditions. Thus Fig. 2 shows that the ratio changes its value from 1 to $\approx$2.4. At this point, the most promising values are 1 and 2. However, the cases when $\omega_1/\omega_2 = 1$ correspond to the situations when $\alpha = 0$ (we have no external excitation) or $\varepsilon \to 0$ (internal interactions between oscillators are neglected), and are not interesting for us. Thus, the cases when $\omega_1/\omega_2 = 2$ seem to be more promising and therefore we shall concentrate on them in this paper. From Fig. 2, we see that the assumed ratio between two frequencies can be achieved for two situations. Indeed, it can be shown that when the strengths of interactions α and ε fulfill the relation

$$
\varepsilon = \frac{12\,\alpha}{10 \pm \sqrt{28}},
\tag{10}
$$

the condition $\omega_1/\omega_2 = 2$ is achieved. For these two situations, our system exhibits periodic behavior with periods T determined by the formula

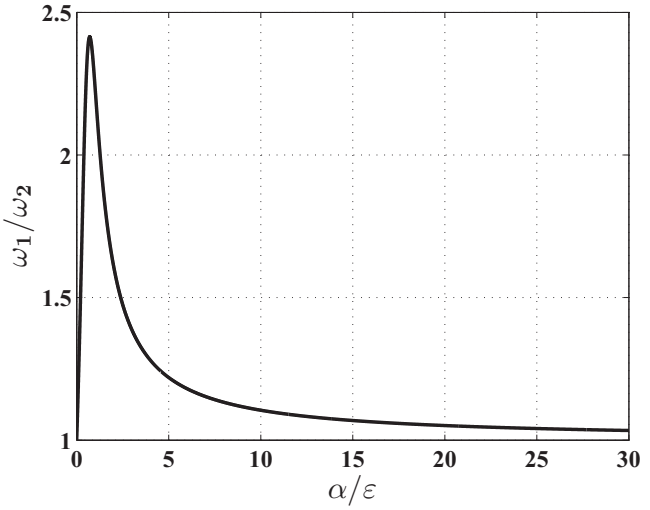

FIG. 2. The ratio ω_1/ω_2 as a function of α/ε calculated from the analytical solution given by Eq. (8).

$$
T = \frac{\sqrt{5 \pm \sqrt{7}}\pi}{2\alpha},
\tag{11}
$$

respectively.

To validate the exactness of the NQS approximation, we have solved the Schrödinger equation numerically, assuming that 10 n-photon states are involved in the evolution for each mode of the field. Next, we have compared numerical results with those derived from our analytical formulas (valid for $2 \otimes 2 \otimes 2$-dimensional Hilbert space). In particular, we have calculated the fidelity between the cut wave function $|\psi\rangle_{\text{cut}}$ defined in Eq. (6) and the "full" wave function obtained from numerical analysis. Thus, Fig. 3 shows the deviation of the fidelity $F(t) = |\langle\psi(t)|\psi(t)\rangle_{\text{cut}}|$ from the unity for one of the two cases in which we are interested. For the second value of ε, $1 - F(t)$ dependence is similar. We see that such deviations are of the order of $\sim 10^{-5}$ and, hence, we can assume that the

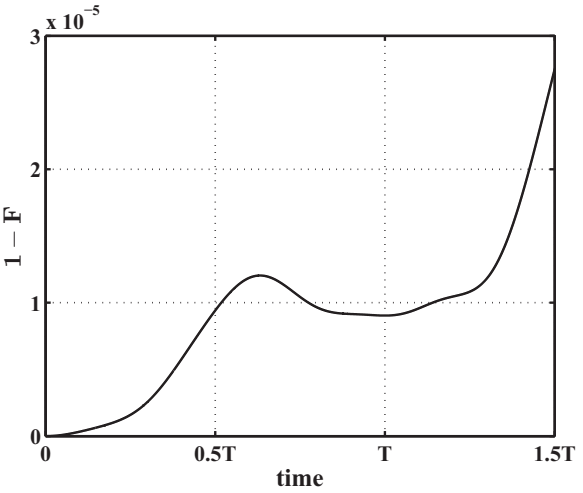

FIG. 3. Time evolution of the parameter $1 - F(t)$ for $\alpha = 0.001\chi$, $\varepsilon = \frac{12\alpha}{10+\sqrt{28}}$. Time is measured in units of $T = \frac{\sqrt{5+\sqrt{7}}\pi}{2\alpha}$.

NQS approximation works well and gives sufficiently accurate results for our purposes.

III. FIRST- AND SECOND-ORDER CORRELATION FUNCTIONS AND TRIPARTITE ENTANGLEMENT

The quantumness of the physical system can be revealed, for example, in the generation of various quantum correlations. We will analyze the quantum properties of the coupled nonlinear system using first and second-order correlation functions ($g^{(1)}$ and $g^{(2)}$), and bi- and tripartite entanglement.

Quantum correlations and their relations to entanglement creation can be found, for example, in considering the atomic ensemble in high-Q cavity [31], an optomechanical system composed of a cavity mode interacting with three bosonic modes obtained in an optical lattice [32], other optomechanical systems such as a cavity with an oscillating mirror and filled with atoms [38], or a nanomechanical resonator coupled to a superconducting microwave cavity mode [39]. It was also suggested there that whenever the first-order correlation (coherence) between the two considered modes is present, there is no entanglement between these modes.

The degree of coherence (amplitude correlation) can be defined with the use of the first-order correlation function [40,41],

$$g_{jk}^{(1)} = \frac{|\langle \hat{a}_j^\dagger \hat{a}_k \rangle|}{\langle \hat{a}_j^\dagger \hat{a}_j \rangle^{\frac{1}{2}} \langle \hat{a}_k^\dagger \hat{a}_k \rangle^{\frac{1}{2}}}, \tag{12}$$

where j,k label the system's modes and when $j \neq k$, the $g^{(1)}$ function describes cross coherence between the two modes. The first-order correlation function takes values from zero to unity. If $g_{jk}^{(1)} = 1$, one can observe coherence between the modes j and k; if it is zero, coherence is not present. Second-order correlation (intensity correlations) is expressed by [40,41]

$$g_{jk}^{(2)} = \frac{\langle \hat{a}_j^\dagger \hat{a}_k^\dagger \hat{a}_j \hat{a}_k \rangle}{\langle \hat{a}_j^\dagger \hat{a}_j \rangle \langle \hat{a}_k^\dagger \hat{a}_k \rangle}. \tag{13}$$

For correlated modes, function $g_{jk}^{(2)}$ takes values greater than unity; for uncorrelated modes, it is equal to unity; and it takes values smaller than unity if the modes are anticorrelated. For the system of the three coupled nonlinear oscillators initially prepared in a vacuum state, and evolving according to the Schrödinger equation, the following relation between the amplitudes is satisfied: $C_{001} = C_{100}$ and $C_{011} = C_{110}$. Due to this symmetry, cross coherence and the second-order correlation function between the boundary and central oscillators (b-c) are equal to each other ($g_{12}^{(1)} = g_{23}^{(1)}$ and $g_{12}^{(2)} = g_{23}^{(2)}$).

As a measure of two-mode entanglement, we apply the one which is based on the negative partial transposition criterion (NPT criterion)—the negativity [42,43]. If $\rho_{ij}^{T_i}$ describes the partial transposition (with respect to i mode) of the density matrix for the system, then the negativity is defined as a sum of absolute values of all the negative eigenvalues calculated for $\rho_{ij}^{T_i}$,

$$N_{ij}(\rho) = \sum_l \mu_l\left(\rho_{ij}^{T_i}\right), \tag{14}$$

where $\rho_{ij} = \mathrm{Tr}_k(\rho_{ijk})$. Negativity is able to distinguish between separable and entangled states for the systems $2 \otimes 2$ or $2 \otimes 3$ and takes values between 0, for separable states, and 1, for maximally entangled ones, for such systems. The evolution of all the discussed types of quantum correlations for bipartite systems is presented in Fig. 4 for the two previously chosen values of ε; see Eq. (10). For both values of coupling ε, the bipartite entanglement is created alternately for b-c oscillators and b-b ones. Therefore, the boundary modes, even though not coupled to each other, can create entangled states via the interactions with the central oscillator. The degree of entanglement between boundary oscillators is not sensitive to the coupling strength ε. On the contrary, the degree of entanglement created by b-c oscillators is directly dependent on ε. By changing the value of internal interactions, one can influence the degree of neighboring bipartite entanglement, and additionally the degree of tripartite entanglement (discussed later).

It is known that intermode correlations of the second order are related to the process of bipartite entangled states creation. In the chain of nonlinear oscillators, the second-order correlations in boundary modes are connected to entanglement between them if these modes are not additionally correlated (or anticorrelated) with the mode of the central oscillator. On the other hand, entanglement between the modes of b-c oscillators can arise if they are anticorrelated and no correlations between the boundary oscillators are present. What is also worth stressing is the relation between the first-order correlation functions and bipartite entanglement mentioned in [32]. In the chain of two-qubit systems, first-order coherence is connected with the lack of entanglement when the system periodically returns to its initial vacuum state (for times distant by one period: T value). During the exchange of entanglement between the pairs of oscillators, one can find that the maximum entanglement between the b-b modes (not directly interacting with each other) is created when there is no coherence between them. The opposite is observed for interacting modes.

The whole system is composed of three oscillators (three modes of the field) and, as it was already shown, each of them can evolve as a two-level system. As a consequence, each oscillator can be treated as a qubit, and the whole system as a three-qubit one. In this section, we will analyze our system's ability to produce tripartite entanglement and identify different classes of three-qubit entangled states.

Whereas the entanglement of bipartite systems is well understood, it is recognized that the entanglement of tripartite quantum states is not a trivial extension of its bipartite counterpart [44].

Dür *et al.* [45] have classified three-qubit states according to their equivalence types under stochastic local operations and classical communication (SLOCC). Thus, they have proposed three classes of the three-qubit states: full separable states (labeled here as I), biseparable states (II), and full tripartite entanglement states (III). On the other hand, for the pure three-qubit states, two inequivalent kinds of tripartite entanglement are distinguished, represented by the GHZ and W states [45]. The GHZ state has only full tripartite entanglement and the entanglement disappears if any one of the three qubits is traced out—the remaining two are always in a separable state. On the other hand, for the W states,

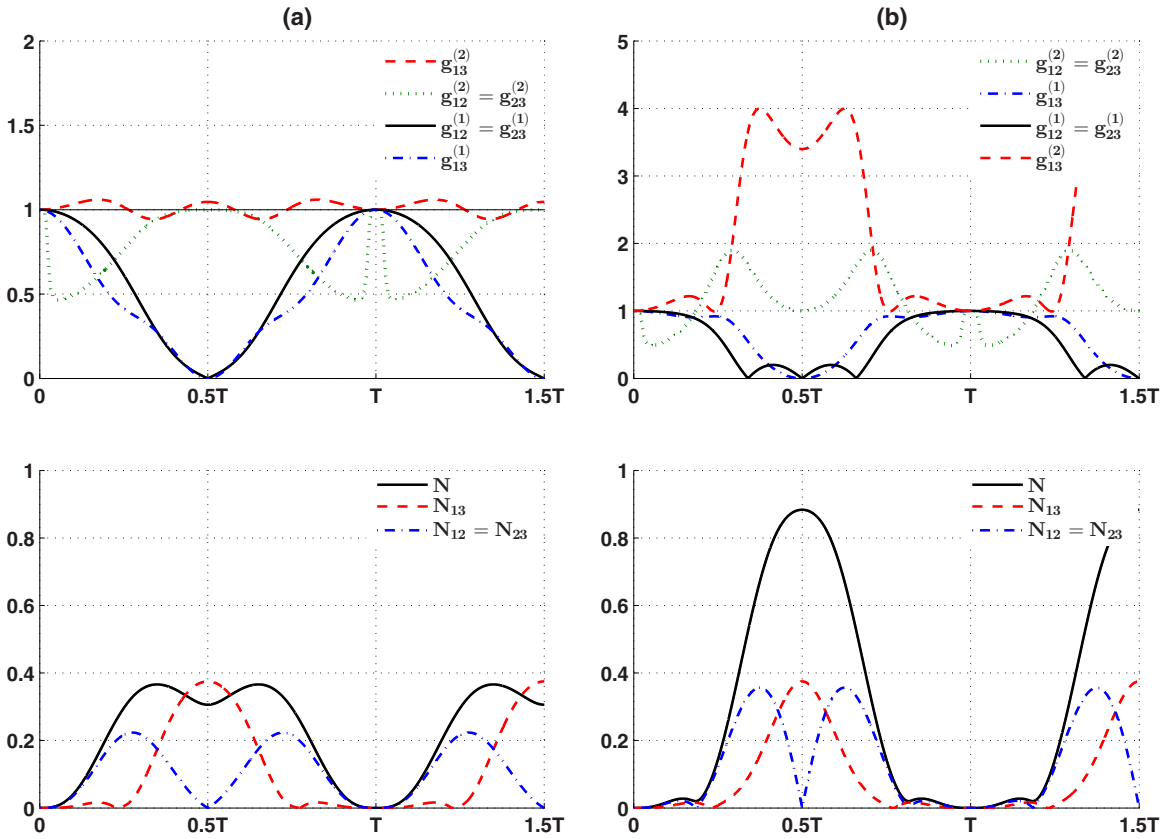

FIG. 4. Time evolution of (a) first-order and second-order correlation function on the top, and reduced (considered here) and tripartite (discussed in the next section) negativities on the bottom for $\alpha = 0.001\chi$, $\varepsilon = \frac{12\alpha}{10+\sqrt{28}}$. (b) The same as in (a), but for $\varepsilon = \frac{12\alpha}{10-\sqrt{28}}$. Time is measured in units of T.

bipartite entanglement is present; and when one of the qubits is removed by the tracing procedure, the other two remain maximally entangled. However, one should keep in mind that the classification proposed in [45] does not include some other states, such as the so-called star-shaped states [46,47]. Therefore, Sabín and García-Alcaine have proposed in [48] an extended classification that includes both pure and mixed states. To be more specific, the classification scheme proposed in [48] divides the class of tripartite entangled states into the following four subtypes:

(i) Subtype III-0 that contains the states for which all bipartite entanglements disappear [all reduced negativities $N_{ij} = 0$; see Eq. (14)]. The well-known representative state belonging to this subtype is the GHZ state. For that reason, the states from this class are called GHZ-like states.

(ii) Subtype III-1 for which only one of the reduced negativities is nonzero, whereas the remaining two are zero valued.

(iii) Subtype III-2 contains star-shaped states for which two reduced negativities have nonzero values.

(iv) Subtype III-3. To this subtype belong the so-called W-like states characterized by three nonzero reduced negativities.

To sum up the above description, all possible classes of the tripartite entanglement and their relation to the reduced bipartite negativities has been presented in Table I. It is worth emphasizing that the Dür *et al.* classification scheme contains states of the two types only. These are types III-0 and III-3.

Now, in order to classify the various types of entanglement which can be generated by the system, we follow the path proposed in [48] applying the geometrical average of three negativities,

$$N(\rho) = (N_{1-23} N_{2-13} N_{3-12})^{\frac{1}{3}}, \tag{15}$$

as a good measure of full tripartite entanglement. The parameters N_{i-jk} are the bipartite negativities for the three-mode density matrix ρ_{ijk}, where the partial transpose is made for the mode (subsystem) i. By contrast to other tripartite entanglement measures (see, for instance, [49,50]), the one defined in (15) is always equal to zero for the states belonging to the classes I and II (according to the classification proposed by Dür *et al.*), and has nonzero values for all subtypes of tripartite entanglement listed above.

The time evolution of negativities describing tripartite entanglement for the two chosen coupling strengths is presented

TABLE I. The types of full tripartite entanglement.

Type of tripartite entanglement	Reduced entanglement	Generated state
III-0	$N_{ij} = N_{jk} = N_{ik} = 0$	GHZ-class state
III-1	$N_{ij} \neq 0,\ N_{jk} = N_{ik} = 0$	
III-2	$N_{ij} \neq 0,\ N_{jk} \neq 0,\ N_{ik} = 0$	starlike state
III-3	$N_{ij} \neq 0,\ N_{jk} \neq 0,\ N_{ik} \neq 0$	W-class state

in Fig. 4. It is seen that for both values of ε, three-qubit entangled states are generated. We have already shown that coupling strength influences the degree of two-qubit entanglement between b-c oscillators, but we may also conclude that this influence on the formation of three-qubit entanglement is more pronounced. Even though Bell-like states are obtained with probabilities that do not exceed 40%, the three-qubit entangled states are obtained (for the same values of the interaction strengths) with probabilities higher than 80%; see Fig. 4.

For both ε values, during the evolution in time, different types of tripartite entangled states can be obtained. For times equal to 0.5 of the oscillation period ($t = 0.5T$), we have identified the entangled state of the whole system as being the III-1 type (Table I)—for those moments of time, only boundary oscillators are entangled, but the system as a whole can be found in an almost maximally entangled state; see Fig. 4. The b-b oscillator pair is correlated and both of the b-c oscillators pairs are not correlated. The entangled W state is generated with a smaller probability; as seen from Fig. 4, all of the two-qubit pairs are entangled and all of them are correlated ($g^{(2)}_{12,23} > 0$ and $g^{(2)}_{13} > 0$).

A smaller interaction between the boundary and central oscillators results in smaller probabilities of the obtained tripartite entangled state; see Fig. 4. For other times, for which one can observe entanglement between all of the oscillators, the system can be found in III-3-type states, i.e., W states. Adequate fidelities corresponding to different three-qubit entangled states are presented in Fig. 5.

For a smaller b-c interaction, when tripartite negativity reaches its maximum, all three reduced negativities are nonzero (III-3 type of tripartite entanglement). We can conclude that this class of tripartite entanglement is associated with production of a W-class state; see Fig. 5(a). As seen from Fig. 4, the W-class state is obtained when all oscillator pairs are anticorrelated. Additionally, the generation of III-1-type states is also connected with second-order correlations present only in the modes corresponding to boundary oscillators. For larger interaction between the oscillators [Fig. 5(b)], the maximum of tripartite entanglement is associated with production of the states $(|0\rangle_2 \pm |1\rangle_2)(|00\rangle_{13} \pm |11\rangle_{13})$.

If we compare our results with the ones presented in [29] for the system of three mutually coupled Kerr-like oscillators with no external excitation, for which the authors reported the possibility of producing entangled W states, we can see that the dynamics in our model is richer and the system is able to produce other types of three-qubit entangled states with high probabilities.

The results presented so far concern the two values of interactions between the neighboring oscillators that correspond to regular and periodic solutions. If the values of ε are different, the evolution of correlation functions and entanglement will be more complicated. But it appears that it is possible to obtain values of negativity describing tripartite entanglement slightly less than unity—meaning that an almost maximally entangled three-qubit state (MES) is generated. That can be obtained by slightly detuning the value of ε from one of the regular solutions. The results are seen in Fig. 6, which presents all of the two-qubit negativities and a three-qubit one [note that the time is scaled in the same units of T, as in Fig. 5(b) for periodic behavior]. The states that are generated

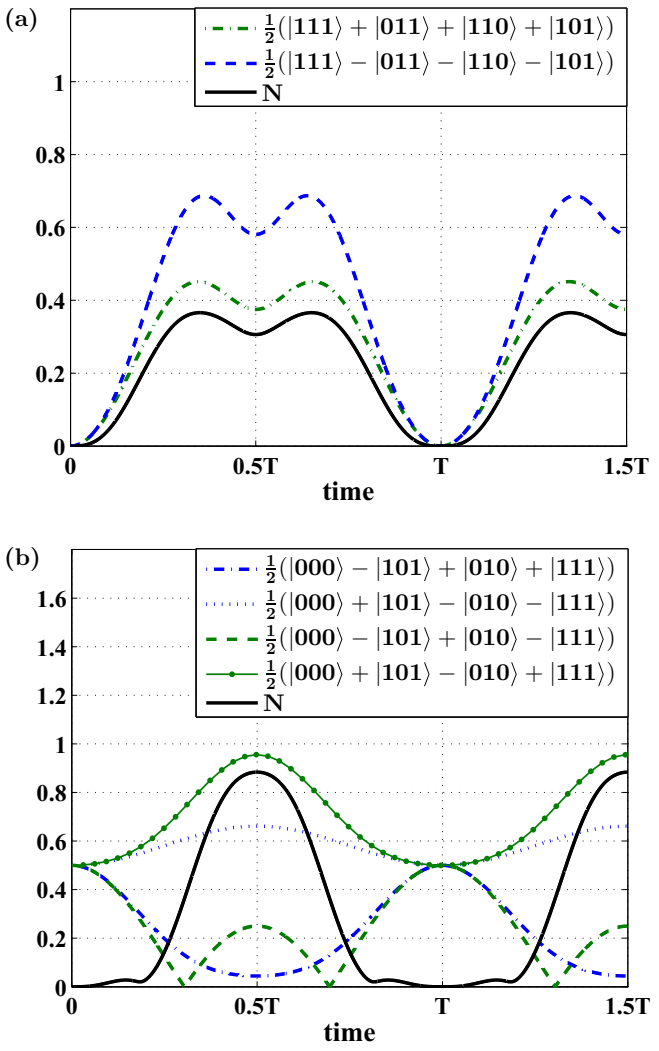

FIG. 5. Time evolution of fidelities corresponding to the same states and tripartite negativity for $\alpha = 0.001\chi$ for (a) $\varepsilon = \frac{12\alpha}{10+\sqrt{28}}$, $T = \frac{\sqrt{5+\sqrt{7}}\pi}{2\alpha}$ and (b) $\varepsilon = \frac{12\alpha}{10-\sqrt{28}}$. Time is measured in units of $T = \frac{\sqrt{5-\sqrt{7}}\pi}{2\alpha}$.

are $\frac{1}{\sqrt{2}}(|000\rangle \pm |111\rangle)$ and $\frac{1}{\sqrt{2}}(|010\rangle \pm |101\rangle)$. Unfortunately, they are slightly perturbed by states $|001\rangle$ and $|100\rangle$ and the result is that we cannot produce a maximally entangled GHZ state (III-0 in Table I) with probability 1. Additionally, once this state is generated, the two-qubit entangled states are produced simultaneously for boundary and between boundary and central oscillators. Due to the fact that they oscillate with slightly different frequencies, in time we will observe the previously mentioned flow of entanglement between the oscillator's pairs and production of other types of three-qubit entangled states.

IV. DAMPED SYSTEM

A. Amplitude damping

In this section, we shall discuss how damping processes influence our system's dynamics. In particular, the time

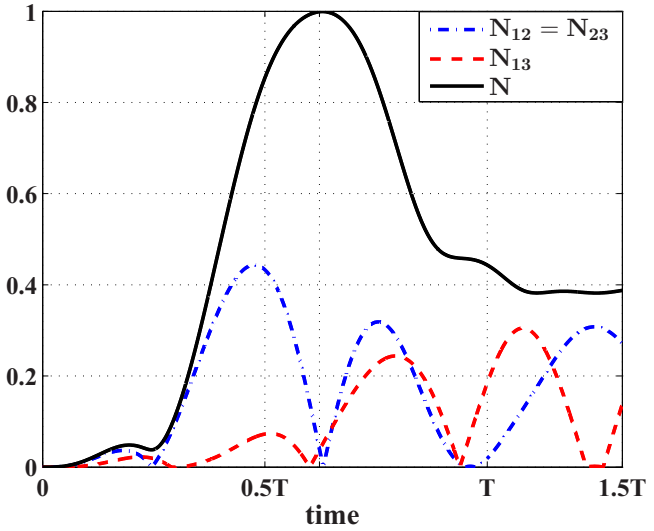

FIG. 6. Time evolution of reduced and tripartite negativities for $\varepsilon = \frac{12\alpha}{10-\sqrt{28}} + \Delta$, $\Delta = -0.6\alpha$. Time is measured in units of the period T, used in Fig. 5(b).

evolution of the first- and second-order correlation functions as well as bi- and tripartite entanglement will be considered.

When amplitude damping is assumed (for the zero-temperature bath), the system's evolution is governed by the following master equation [41,51]:

$$\frac{d\hat{\rho}}{dt} = -\frac{1}{i}(\hat{\rho}\hat{H} - \hat{H}\hat{\rho}) + \sum_{j=1}^{3} \frac{\kappa_j}{2}(2\hat{a}_j\hat{\rho}\hat{a}_j^\dagger - \hat{a}_j^\dagger\hat{a}_j\hat{\rho} - \hat{\rho}\hat{a}_j^\dagger\hat{a}_j), \tag{16}$$

where we have introduced damping parameter κ_j ($j = 1,2,3$) describing the interaction with a zero-temperature bath for the modes 1, 2, and 3, respectively. For simplicity, we assume that all damping parameters appearing here are the same for all of the modes, i.e., $\kappa_1 = \kappa_2 = \kappa_3 = \kappa$ and $\kappa = 0.1\alpha$. The same as for the cases discussed in previous sections, the system is excited in two modes and $\alpha = 0.001\chi$ (only boundary oscillators 1 and 3 are excited). Moreover, since the results corresponding to the two considered values of the excitation strength ε are very similar to each other, we shall concentrate on the case when $\varepsilon = \frac{12\alpha}{10-\sqrt{28}}$ (stronger internal interaction case). We shall mostly discuss two cases: one corresponding to the periodic solution, i.e., for $\varepsilon = 12\alpha/(10-\sqrt{28})$, and the second which corresponds to the situation presented in Fig. 6, when $\varepsilon = 12\alpha/(10-\sqrt{28}) + \Delta$ and the system exhibits quasiperiodic behavior.

When our system is influenced by an external zero-temperature bath, its behavior changes considerably from that corresponding to the nondamped cases. In Fig. 7, we show the time evolution of the negativities describing both bi- and tripartite entanglement ($\{N_{12} = N_{23}, N_{13}\}$ and N, respectively). Figure 7(a) corresponds to the case when $\omega_1 = 2\omega_2$, i.e., the system evolves periodically, whereas Fig. 7(b) shows the system's evolution when internal coupling constant ε is slightly perturbed by $\Delta = -0.6\alpha$ (for such situation, we get maximal value for the tripartite negativity for the nondamped case;

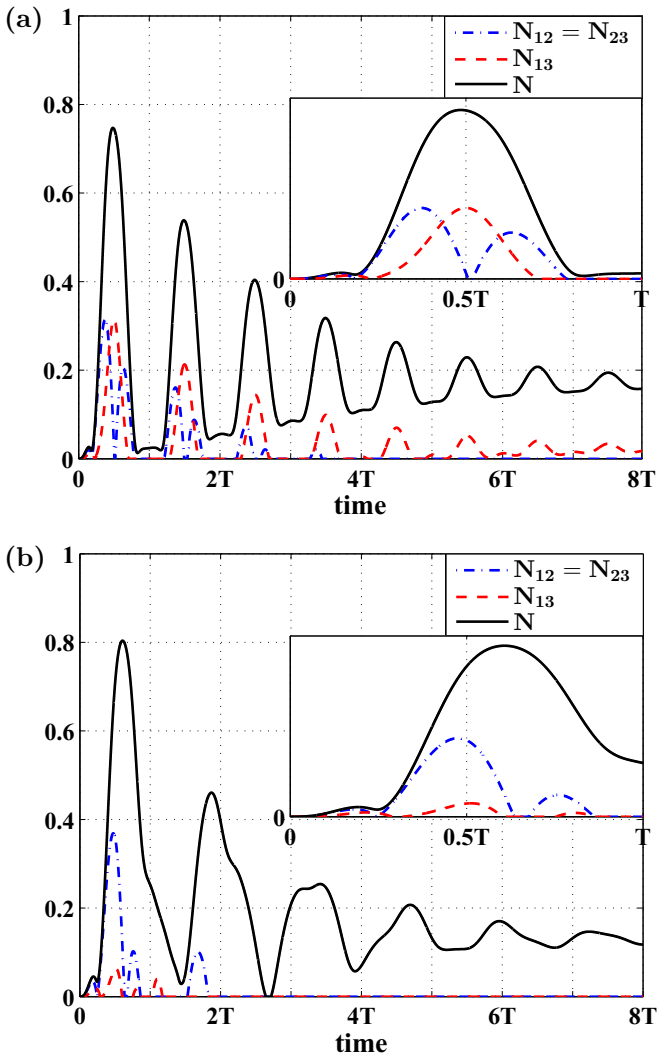

FIG. 7. Time evolution of the reduced and tripartite negativities for $\alpha = 0.001\chi$, (a) $\varepsilon = \frac{12\alpha}{10-\sqrt{28}}$, (b) $\varepsilon = \frac{12\alpha}{10-\sqrt{28}} + \Delta$, where $\Delta = -0.6\alpha$. The amplitude-damping parameter $\kappa = 0.1\alpha$. Time is measured in units of $T = \frac{\sqrt{5-\sqrt{7}}\pi}{2\alpha}$.

see Fig. 6). Moreover, when the internal coupling constant is perturbed, our system exhibits quasiperiodic evolution. Thus, we see that N exhibits damped oscillations and tends to its final nonzero value ($\sim$0.16). It differs from zero, so tripartite entanglement does not disappear during the entire time of the system's evolution. Moreover, the maximal value of N is reached for the time $t = T/2$ and its value $\sim$0.7. At the same moment of time, N_{13} also becomes maximal ($\sim$0.3), whereas $N_{12} = N_{13}$ are equal to zero. In consequence, we do not observe bipartite entanglement between neighboring oscillators, whereas the entanglement between two boundary oscillators reaches its maximum (one should remember that it does not mean that we generate a maximally entangled state here). For such a situation, the state of the III-1 type is generated. It is the state $|0\rangle_2 \pm |1\rangle_2)(|00\rangle_{13} \pm |11\rangle_{13})$ with some addition of the states $|001\rangle$, $|100\rangle$, $|011\rangle$, and $|110\rangle$, and hence maximal value of $N < 1$. Moreover, we observe the sudden death of entanglement [52] and its rebirth [53] for all

cases of bipartite entanglement represented by the negativities N_{ij} ($i = \{1,2\}$, $j\{2,3\}$). In the long-time limit, we see that final values of the negativities N and N_{13} reach some nonzero values, whereas the entanglement represented by $N_{12} = N_{23}$ disappears.

When the internal coupling is equal to $\frac{12\alpha}{10-\sqrt{28}} + \Delta$, where $\Delta = -0.6\alpha$ [Fig. 7(b)], we see behavior similar to that observed for the situation presented in Fig. 7(a). For this case, we observe slightly greater value of the maximum of $N \simeq 0.8$ and damped oscillations of all negativities. As in the previous case, the sudden death of bipartite entanglement and its rebirth represented by all reduced negativities are present in the system's evolution, and N tends to its final nonzero value again. However, due to the fact that two slightly different frequencies govern the time evolution of the model, some dephasing appears in the system, and when N reaches its first maximum, all of the reduced negativities become practically equal to zero. Consequently, this maximum of N corresponds to the generation of the tripartite entangled state of the type III-0, contrary to the situation depicted in Fig. 7(a), where the entanglement of type III-1 was present. Moreover, we see that for time $t \to \infty$, all reduced negativities describing bipartite entanglement tend to zero.

Quantum correlations and, hence, the characteristics of our system's steady state strongly depend on the value of the damping constant. Thus, Fig. 8 shows the dependence of all negativities considered here and correlation functions on the value of κ (expressed in the units of external coupling α). Figure 8(a) depicts how first- and second-order intermode correlation functions change their final values with increasing value of κ (for the periodic and quasiperiodic cases, those dependences are almost identical). We see that for the very weak damping case, all $g^{(1)}$ functions are close to zero, so we do not observe first-order correlations. However, as κ increases, when $\kappa/\alpha >\sim 5$, all functions practically become equal to unity. If we look at second-order correlations, the situation is more complicated. For small values of κ, they are greater than 1 and we observe intermode anticorrelations for all modes of the field. Those anticorrelations increase to reach their maximal values and then start to fall down with increasing κ. For the correlations between the two boundary oscillators' modes (1 and 3), some range of the values of κ exists for which anticorrelations are observed. However, for $\kappa >\sim 5$, we observe tiny and vanishing correlations again. Correlations between two neighboring modes ($1-2$ and $2-3$) reach their maximum for greater value of κ if we compare it with that corresponding to the maximal value of $g^{(2)}_{13}$. Then, the values of $g^{(2)}_{12}$ and $g^{(2)}_{23}$ decrease and become negative for the same value of κ when anticorrelations between the modes $1-3$ disappear. What is interesting is that although the correlations described by $g^{(2)}_{13}$ practically disappear for stronger damping, anticorrelations described by $g^{(2)}_{12}$ and $g^{(2)}_{23}$ remain in the system even for large values of κ.

Figures 8(b) and 8(c) show long-time values of the tri- and bipartite negativities, corresponding to the various values of damping constant κ (expressed in the units of external coupling strength α). Figure 8(b) corresponds to the case when the system's dynamics is periodic ($\varepsilon = \frac{12\alpha}{10-\sqrt{28}}$), whereas for the situation presented in Fig. 8(c), internal coupling strength

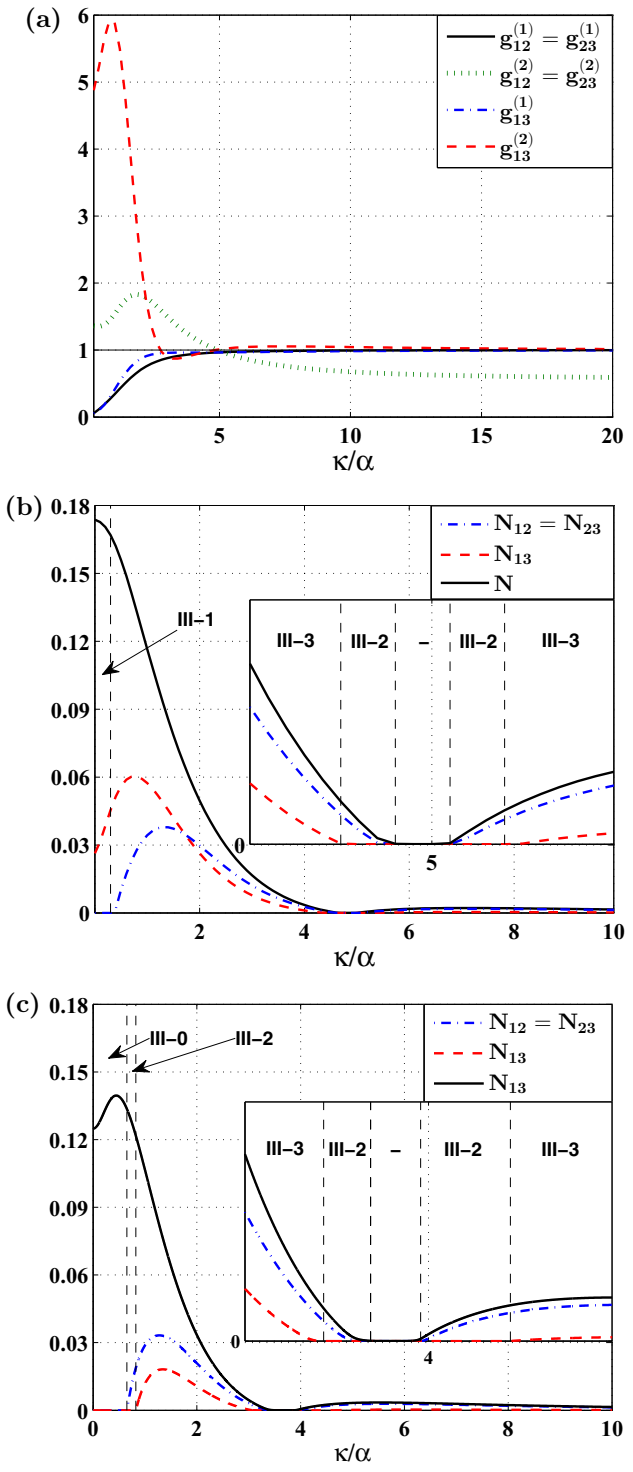

FIG. 8. Steady-state solutions for (a) the intermode correlation functions $g^{(1)}$ and $g^{(2)}$ and for the negativities (full tripartite N and reduced bipartite N_{ij}) vs the value of the damping parameter where (a),(b) $\varepsilon = \frac{12\alpha}{10-\sqrt{28}}$ and (c) $\varepsilon = \frac{12\alpha}{10-\sqrt{28}} + \Delta$ ($\Delta = -0.6\alpha$). The external coupling strength $\alpha = 0.001\chi$.

is perturbed, i.e., $\varepsilon = \frac{12\alpha}{10-\sqrt{28}} + \Delta$, where $\Delta = -0.6\alpha$ (for this case, our system exhibits quasiperiodic behavior). In Fig. 8(b), we see that although the tripartite entanglement decreases with growing value of κ (when $\kappa/\alpha <\sim 4.5$), the

TABLE II. Different types of full tripartite entanglement generated for a long-time limit for the cases when (a) $\varepsilon = \frac{12\alpha}{10-\sqrt{28}}$ and (b) $\varepsilon = \frac{12\alpha}{10-\sqrt{28}} + \Delta$, where $\Delta = -0.6\alpha$.

Damping parameter	Type of tripartite entanglement
(a)	
$\kappa < 0.4\alpha$	III-1
$0.4\alpha < \kappa < 4.5\alpha$	III-3
$4.5\alpha < \kappa < 4.8\alpha$	III-2
$4.8\alpha < \kappa < 5.1\alpha$	
$5.1\alpha < \kappa < 5.4\alpha$	III-2
$\kappa > 5.4\alpha$	III-3
(b)	
$\kappa < 0.65\alpha$	III-0
$0.65\alpha < \kappa < 0.82\alpha$	III-2
$0.82\alpha < \kappa < 3.14\alpha$	III-3
$3.14\alpha < \kappa < 3.53\alpha$	III-2
$3.53\alpha < \kappa < 3.94\alpha$	
$3.94\alpha < \kappa < 4.67\alpha$	III-2
$\kappa > 4.67$	III-3

negativities describing bipartite entanglement can increase for such situation, and for some values of the damping constant they reach their maximal values. When $\kappa/\alpha <\sim 5.4$ [see Table II and the inset in Fig. 8(b)], three various classes of the tripartite entangled states can be generated depending on the value of κ, and for $\kappa/\alpha \simeq 5$, no entanglement is produced—all the negativities are equal to zero. In general, if we look at the values of the negativities describing two- ($N_{12} = N_{23}$, N_{13}) and tripartite (N) entanglement, we can identify various regions for which one or more of them are equal to zero. Thus, we can identify various classes of tripartite entangled states corresponding to different values of κ (Table II shows approximate values of κ for which the steady states of our system belong to various classes of the tripartite entangled state). In particular, for the situation presented in Fig. 8(b), they are III-1, III-2 (starlike), and III-3 (W-class) states. It is seen from Fig. 8(b) that the highest values of all bipartite negativities can be found when $\sim 0.5\kappa/\alpha < \sim 2$. For such a situation, tripartite negativity N is relatively high as well, so the W state can be generated with better efficiency than for the cases when other classes of states are produced. Nevertheless, applying various strengths of damping, we can switch the final system's state from one belonging to the particular class to another.

Figure 8(c) corresponds to the situation when internal coupling ε is perturbed, i.e., $\varepsilon = \frac{12\alpha}{10-\sqrt{28}} + \Delta$ ($\Delta = -0.6\alpha$). For such situation, the system evolves quasiperiodically and, hence, we observe some dephasing effect as a result of the appearance of two different frequencies in the system's dynamics. Consequently, different types of the bipartite entanglement represented by the reduced negativities disappear (or reappear) for different values of κ/α as we compare them with their counterparts from Fig. 8(b), and other types of the entangled states are generated [see Table II(b)]. We see that our system is able to produce various types of tripartite entanglement and is fragile on the values of the parameters describing it. So, by the appropriate tuning of the parameters, we can switch the final state of the system from one kind of state to another. Moreover, what is interesting is that for the weak damping case, tripartite negativity can increase with growing value of κ/α. When we observe this feature, bipartite entanglement is absent—reduced negativities are equal to zero. Moreover, as seen in Figs. 8(b) and 8(c), there exists for both cases some range of the values of the damping constant for which the final state of the system is not entangled—all of the negativities describing tri- and bipartite entanglement are equal to zero.

B. Phase damping

In this section, we consider the influence of phase damping on the generation of various tripartite entangled states. When we include phase-damping effects, the system does not lose its energy and populations of the states represented by diagonal matrix elements do not decay. For such cases, decoherence effects and, hence, entanglement losses can be observed. This is an effect of decay of other than diagonal matrix elements. Decoherence induced by the phase-damping reservoir is related to random changes in the relative phases of superposed states during the system's time evolution. Moreover, dephasing processes can lead to other interesting phenomena, such as sudden death of entanglement and/or its reappearing.

To describe phase-damping effects, we apply the following master equation [41,51]:

$$\frac{d\hat{\rho}}{dt} = -\frac{1}{i}(\hat{\rho}\hat{H} - \hat{H}\hat{\rho}) + \sum_{j=1}^{3}\frac{\kappa_j}{2}[2\hat{a}_j^\dagger\hat{a}_j\hat{\rho}\hat{a}_j^\dagger\hat{a}_j - (\hat{a}_j^\dagger\hat{a}_j)^2\hat{\rho} - \hat{\rho}(\hat{a}_j^\dagger\hat{a}_j)^2], \quad (17)$$

where κ_j ($j = \{1,2,3\}$) is a damping parameter corresponding to the modes 1, 2, and 3, respectively. Analogously, as for the cases discussed in the previous section where the system was amplitude damped, we assume here that damping parameters are the same for all modes $\kappa_1 = \kappa_2 = \kappa_3 = \kappa$ and are equal to 0.1α, and the excitation strength $\alpha = 0.001\chi$. Moreover, we consider two cases when the internal coupling parameter $\varepsilon = \frac{12\alpha}{10-\sqrt{28}}$ and $\varepsilon = \frac{12\alpha}{10-\sqrt{28}} + \Delta$ ($\Delta = -0.6\alpha$), as in the previous cases.

Thus, Fig. 9(a) shows the time evolution of all the negativities considered here when $\varepsilon = \frac{12\alpha}{10-\sqrt{28}} + \Delta$ ($\Delta = -0.6\alpha$) (the system evolves periodically). It is seen that thanks to the presence of the phase damping, both effects, i.e., sudden death of entanglement and entanglement revival, are present in the system. These two phenomena can be observed for the bipartite and tripartite entanglement as well. In a long-time limit, all negativities disappear, so the entanglement of any kind does not survive, contrary to the case of the amplitude damping discussed in the previous section (see nonzero values of the negativities for the steady state in Fig. 8). In this limit, all eight states involved in the system's evolution are equally populated with the same probability equal to 0.125.

Nevertheless, for shorter times, a considerable amount of tripartite entanglement can be generated. For $t = T/2$, tripartite negativity N reaches its greatest maximum and slightly exceeds 0.8. At the same moment of time, reduced negativity N_{13} becomes maximal, whereas the negativities

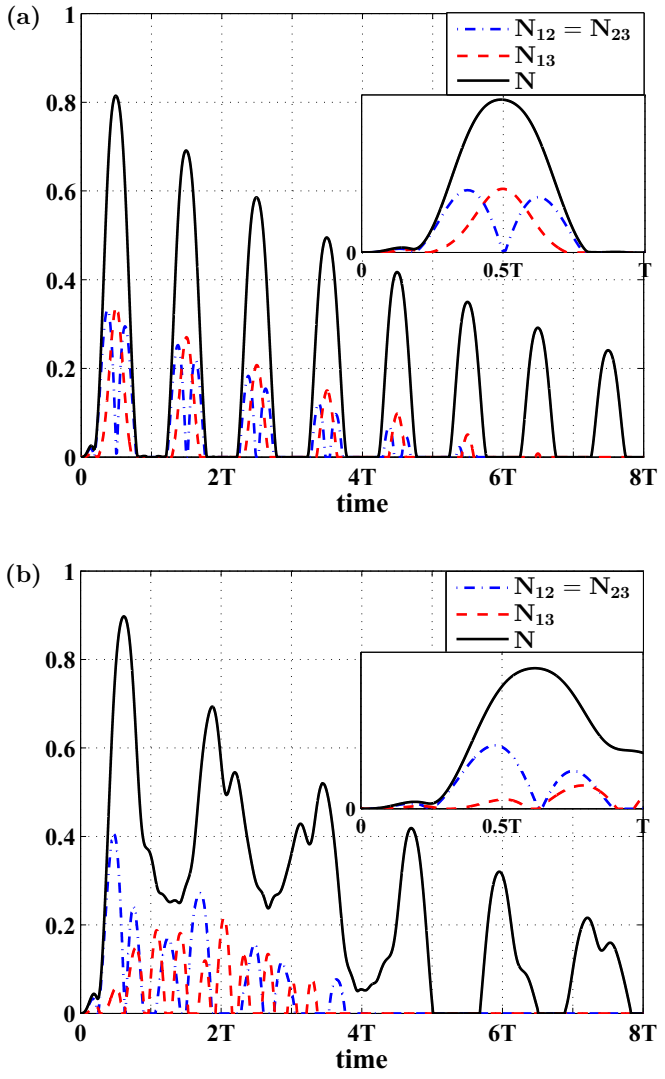

FIG. 9. Time evolution of the reduced and tripartite negativities for (a) $\varepsilon = \frac{12\alpha}{10-\sqrt{28}}$ and (b) $\varepsilon = \frac{12\alpha}{10-\sqrt{28}} + \Delta$, where $\Delta = -0.6\alpha$. Time is measured in units of $T = \frac{\sqrt{5-\sqrt{7}}\pi}{2\alpha}$, phase-damping parameter $\kappa = 0.1\alpha$, and $\alpha = 0.001\chi$.

$N_{12} = N_{23}$ describing entanglement between two neighboring oscillators (modes) become equal to zero. For such situation, we generate the III-1 class state $|0\rangle_2 \pm |1\rangle_2)(|00\rangle_{13} \pm |11\rangle_{13})$, which is slightly perturbed by $|001\rangle$, $|100\rangle$, $|011\rangle$, and $|110\rangle$. Thanks to the periodic evolution of the system, at the next maxima of N, we see the similar situation, although the degree of the entanglement becomes smaller and smaller as we reach successive maxima. Additionally, when all of the reduced negativities describing bipartite entanglement differ from zero and $N \neq 0$ as well, W-type states are generated. When we decrease internal coupling ($\varepsilon = \frac{12\alpha}{10-\sqrt{28}} + \Delta$ where $\Delta = -0.6\alpha$), we observe a similar behavior of our system, albeit some irregularities appear in the time evolution of the negativities. Moreover, analogously to the situation depicted in Fig. 7, the maximal value of N describing tripartite entanglement increases and becomes equal to $\simeq 0.9$. What is interesting is that all reduced negativities N_{ij} ($\{i,j\} = \{1,2,3\}$) after some period of time when they exhibit irregular oscillations (for $t > \sim 4T$) become equal to zero, and we observe sudden death of bipartite entanglement without its revival.

V. SUMMARY

We have discussed the model of a chain of three nonlinear oscillators excited by two external coherent fields. In particular, we were interested in a time evolution of the quantum correlations present in the system and the possibility of generation of the entangled quantum states, which are especially interesting from the point of view of quantum information theory. As the model consists of the three oscillators, we have discussed both the bi- and tripartite entanglement.

We have shown that under some conditions, our model can be treated as *nonlinear quantum scissors* and evolves within a set of eight states $|ijk\rangle$, where $\{i,j,k\} = \{0,1\}$. As a consequence, the system considered here can be treated as a three-qubit system. We have shown that such system can be a source of entangled two-qubit and three-qubit states, including maximally entangled ones. For the case of the two-qubit entanglement, one can observe not only its flow between the pairs of oscillators, but also that the entanglement can be created even between two oscillators which are not directly coupled together. We have also discussed the connections between the first- and second-order correlation functions, and various relations between those correlations and creation of the entanglement.

The possibility of creation of tripartite entanglement in our model was discussed as well. It has been shown that it is possible to obtain an almost maximally entangled three-qubit state if only the pair of externally excited oscillators is entangled, and we observe only second-order correlations between the modes corresponding to these two oscillators. Moreover, the states of W type are created if all the two-qubit subsystems are entangled and $g^{(2)}$ functions indicate either correlations for all subsystems or anticorrelations for all of them. We have shown that it is also possible to generate the state which is very close to the GHZ state.

We have also considered long-time solutions and discussed their dependence on the strength of damping effects. For the amplitude-damping case, we can observe sudden death of the bipartite entanglement and its sudden revivals, whereas for the phase-damping case, the phenomenon of sudden death can be observed for both the bi- and tripartite entanglement.

What is most important is that different classes of tripartite entangled states can be obtained in a stationary state limit, and the type of the final entangled state strongly depends on the values of the parameters describing the system. Consequently, we can "switch" the final state of the system by adiabatic tuning these parameters. Moreover, there is a range of damping constant values for which none of the three-qubit entangled states (and none of two-qubit ones) is created in the steady-state limit.

We believe that all of those facts and the generality of our model allows for the conclusion that physical systems governed by the effective Hamiltonian describing our model can be not only a potential source of various bi- and tripartite entangled states, but also an interesting finding concerning various types of quantum correlations and the relations among them.

ACKNOWLEDGMENTS

W.L. acknowledges the Vietnam Ministry of Education and Training Grant No. B2014-42-29 for support. W.L. would like to thank Professor Ryszard Horodecki for his stimulating questions and discussion concerning sudden death of entanglement for tripartite systems.

[1] M. Stobińska, A. S. Villar, and G. Leuchs, Europhys. Lett. **94**, 54002 (2011).

[2] A. Miranowicz, R. Tanaś, and S. Kielich, Quantum Opt. **2**, 253 (1990).

[3] M. Paprzycka and R. Tanaś, Quantum Opt. **4**, 331 (1992).

[4] M. Stobińska, H. Jeong, and T. C. Ralph, Phys. Rev. A **75**, 052105 (2007).

[5] W. Leoński, Physica A **233**, 365 (1996); P. Szlachetka, K. Grygiel, and M. Misiak, Chaos Solitons Fractals **27**, 673 (2006); A. Kowalewska-Kudłaszyk, J. K. Kalaga, and W. Leoński, Phys. Rev. E **78**, 066219 (2008); Phys. Lett. A **373**, 1334 (2009); K. Grygiel and I. Śliwa, Nonlinear Dynamics **67**, 755 (2012); A. Kowalewska-Kudłaszyk, J. K. Kalaga, W. Leoński, and V. Cao Long, Phys. Lett. A **376**, 1280 (2012); A. R. Shahinyan, L. Y. Chew, and G. Y. Kryuchkyan, *ibid.* **377**, 2743 (2013); T. V. Gevorgyan, A. R. Shahinyan, L. Y. Chew, and G. Y. Kryuchkyan, Phys. Rev. E **88**, 022910 (2013).

[6] S. Bose, K. Jacobs, and P. L. Knight, Phys. Rev. A **56**, 4175 (1997).

[7] K. Jacobs, Phys. Rev. Lett. **99**, 117203 (2007).

[8] M. Stobińska, G. J. Milburn, and K. Wódkiewicz, Phys. Rev. A **78**, 013810 (2008).

[9] Y. X. Liu, A. Miranowicz, Y. B. Gao, J. Bajer, C. P. Sun, and F. Nori, Phys. Rev. A **82**, 032101 (2010).

[10] P. Rabl, Phys. Rev. Lett. **107**, 063601 (2011).

[11] H. Wang, X. Gu, Y. X. Liu, A. Miranowicz, and F. Nori, Phys. Rev. A **92**, 033806 (2015).

[12] L. A. Wu, A. Miranowicz, X. B. Wang, Y. X. Liu, and F. Nori, Phys. Rev. A **80**, 012332 (2009).

[13] A. Barasiński, W. Leoński, and T. Sowiński, J. Opt. Soc. B **31**, 1845 (2014).

[14] R. Islam, R. Ma, P. M. Preiss, M. E. Tai, A. Lukin, M. Rispoli, and M. Greiner, Nature (London) **528**, 77 (2015).

[15] V. Peřinová, A. Lukš, and J. Křapelka, J. Phys. B: At. Mol. Opt. Phys. **46**, 195301 (2013); M. K. Olsen, Phys. Rev. A **92**, 033627 (2015); J. Opt. Soc. Am. B **32**, A15 (2015).

[16] P. Preiss, R. Ma, M. Tai, A. Lukin, M. Rispoli, P. Zupancic, Y. Lahni, R. Islam, and M. Greiner, Science **347**, 1229 (2015).

[17] M. Boissonneault, J. M. Gambetta, and A. Blais, Phys. Rev. A **79**, 013819 (2009).

[18] S. Rebic, J. Twamley, and G. J. Milburn, Phys. Rev. Lett. **103**, 150503 (2009).

[19] A. J. Hoffman, S. J. Srinivasan, S. Schmidt, L. Spietz, J. Aumentado, H. E. Tureci, and A. A. Houck, Phys. Rev. Lett. **107**, 053602 (2011); N. Didier, S. Pugnetti, Y. M. Blanter, and R. Fazio, Phys. Rev. B **84**, 054503 (2011).

[20] N. Korolkova and J. Peřina, Opt. Commun. **136**, 135 (1997); J. Mod. Opt. **44**, 1525 (1997); G. Ariunbold and J. Peřina, Opt. Commun. **176**, 149 (2000).

[21] J. Peřina Jr. and J. Peřina, in *Progress in Optics*, edited by E. Wolf (Elsevier, Amsterdam, 2000), Vol. 41, p. 361.

[22] W. Leoński and A. Miranowicz, J. Opt. B **6**, S37 (2004); A. Miranowicz and W. Leoński, *ibid.* **39**, 1683 (2006); A. Kowalewska-Kudłaszyk and W. Leoński, Phys. Rev. A **73**, 042318 (2006); A. Kowalewska-Kudłaszyk, W. Leoński, and J. Peřina Jr., *ibid.* **83**, 052326 (2011).

[23] W. Leoński and A. Kowalewska-Kudłaszyk, in *Progress in Optics*, edited by E. Wolf (Elsevier, 2011), Vol. 56, p. 131.

[24] A. Kowalewska-Kudłaszyk, W. Leoński, and J. Peřina Jr., Phys. Scr. **2012**, 014016 (2012).

[25] K. M. Birnbaum, A. Boca, R. Miller, A. D. Boozer, T. E. Northup, and H. J. Kimble, Nature (London) **436**, 87 (2005).

[26] A. Faraon, I. Fushman, D. Englund, N. Stoltz, P. Petroff, and J. Vučković, Nat. Phys. **4**, 859 (2008).

[27] C. Lang, D. Bozyigit, C. Eichler, L. Steffen, J. M. Fink, A. A. Abdumalikov, M. Baur, S. Filipp, M. P. da Silva, A. Blais, and A. Wallraff, Phys. Rev. Lett. **106**, 243601 (2011).

[28] I. Bretheau, P. Campagne-Ibercq, E. Flurin, F. Mallet, and B. Huard, Science **348**, 776 (2015).

[29] R. S. Said, M. R. B. Wahiddin, and B. A. Umarov, J. Phys. B: At. Mol. Opt. Phys. **39**, 1269 (2006).

[30] P. Xue, Z. Ficek, and B. C. Sanders, Phys. Rev. A **86**, 043826 (2012); S. Piano and G. Adesso, Entropy **15**, 1875 (2013); Y.-D. Wang, S. Chesi, and A. A. Clerk, Phys. Rev. A **91**, 013807 (2015); S. Armstrong, M. Wang, R. Y. Teh, Q. Gong, Q. He, J. Janousek, H.-A. Bachor, M. D. Reid, and P. K. Lam, Nat. Phys. **11**, 167 (2015).

[31] L. Sun, G. Li, W. Gu, and Z. Ficek, New J. Phys. **13**, 093019 (2011).

[32] L. H. Sun, G. X. Li, and Z. Ficek, Phys. Rev. A **85**, 022327 (2012).

[33] R. Szczęśniak and A. Durajski, Supercond. Sci. Technol. **27**, 015003 (2014); A. Durajski and R. Szczęśniak, *ibid.* **27**, 115012 (2014); D. Szczęśniak, A. Durajski, and R. Szczęśniak, J. Phys.: Condens. Matter **26**, 255701 (2014); A. Durajski, D. Szczęśniak, and R. Szczęśniak, Solid State Commun. **200**, 17 (2014).

[34] W. Leoński and R. Tanaś, Phys. Rev. A **49**, R20 (1994).

[35] A. Miranowicz, W. Leoński, and N. Imoto, in *Modern Nonlinear Optics*, edited by M. Evans (Wiley, New York, 2001), p. 155; W. Leoński and A. Miranowicz, *ibid.*, p. 195.

[36] A. Imamoğlu, H. Schmidt, G. Woods, and M. Deutsch, Phys. Rev. Lett. **79**, 1467 (1997); P. Grangier, D. F. Walls, and K. M. Gheri, *ibid.* **81**, 2833 (1998); A. Miranowicz, M. Paprzycka, Y. X. Liu, J. Bajer, and F. Nori, Phys. Rev. A **87**, 023809 (2013); A. Miranowicz, J. Bajer, M. Paprzycka, Y. X. Liu, A. M. Zagoskin, and F. Nori, *ibid.* **90**, 033831 (2014);

[37] W. Leoński, S. Dyrting, and R. Tanaś, J. Mod. Opt. **44**, 2105 (1997).

[38] H. Ian, Z. R. Gong, Y. X. Liu, C. P. Sun, and F. Nori, Phys. Rev. A **78**, 013824 (2008).

[39] D. Vitali, P. Tombesi, M. J. Woolley, A. C. Doherty, and G. J. Milburn, Phys. Rev. A **76**, 042336 (2007).

[40] C. C. Gerry and P. L. Knight, *Introductory Quantum Optics* (Cambridge University Press, Cambridge, 2005).
[41] D. F. Walls and G. J. Milburn, *Quantum Optics*, 2nd ed. (Springer-Verlag, Berlin, 2008).
[42] A. Peres, Phys. Rev. Lett. **77**, 1413 (1996).
[43] M. Horodecki, P. Horodecki, M. Horodecki, and R. Horodecki, Phys. Lett. A **223**, 1 (1996).
[44] R. Horodecki, P. Horodecki, M. Horodecki, and K. Horodecki, Rev. Mod. Phys. **81**, 865 (2009).
[45] W. Dür, G. Vidal, and J. I. Cirac, Phys. Rev. A **62**, 062314 (2000).
[46] M. Plesch and V. Bužek, Phys. Rev. A **67**, 012322 (2003).
[47] M. Plesch and V. Bužek, Phys. Rev. A **68**, 012313 (2003).
[48] C. Sabin and G. Garcia-Alcaine, Eur. Phys. J. D **48**, 435 (2008).
[49] C. Yu and H. Song, Phys. Lett. A **330**, 377 (2004).
[50] Z. Ma, Z. Chen, and S.-M. Fei, Phys. Rev. A **90**, 032307 (2014).
[51] C. W. Gardiner and P. Zoller, *Quantum Noise* (Springer-Verlag, Berlin, 2010).
[52] K. Życzkowski, P. Horodecki, M. Horodecki, and R. Horodecki, Phys. Rev. A **65**, 012101 (2001); T. Yu and J. H. Eberly, Phys. Rev. Lett. **93**, 140404 (2004); M. Ikram, F. L. Li, and M. S. Zubairy, Phys. Rev. A **75**, 062336 (2007); M. Bartkowiak, A. Miranowicz, X. Wang, Y. X. Liu, W. Leoński, and F. Nori, *ibid.* **83**, 053814 (2011).
[53] Z. Ficek and R. Tanaś, Phys. Rev. A **74**, 024304 (2006); F. Benatti and R. Floreanini, J. Phys. A: Math. Gen. **39**, 2689 (2006); Z. Ficek and R. Tanaś, Phys. Rev. A **77**, 054301 (2008).